THEORETICAL AND APPLIED MECHANICS
23, pp. 1-34, 1997, UDK 532.517.4

Simplified turbulent boundary layer calculation and the transformation of the velocity profile near the separation point

R. Ašković

Submitted 1 November 1996

Abstract

The planar turbulent boundary layer is analyzed in the sense of the well known phenomenologic semi-empiric boundary layer theory. The analysis is based on an analogy with the rheological power laws widely used in the study of non-linear viscous flows. A simple "one layer method" to calculate the turbulent boundary layer is first derived and after that tested on the sphere as well as on the id. 2500 of P.Bradshow. Furthermore, an approximate procedure is proposed to evaluate the evolution of the velocity profile in a neighborhood of the separation point of the turbulent boundary layer in the case of the Prandtl turbulence model. It is assumed that the equations of the boundary layer admit two solutions around the separation point. One of them is upstream of the point and another one downstream of it. The solutions are found in two variants - triangular and parabolic - relative to the method used to approximate the Reynolds' turbulent stress. Besides, a comparison is made with respect to the existing experimental results.

1 Introduction

There has existed since 1977 (Novozilov [1]) a new variant of the phenomenologic semi-empiric turbulent boundary layer theory that is founded on the analogy with the rheologic power laws largely utilized in the study of non-newtonian non-linear flows and on the use of the Kàrmàn turbulence model. It is to note also that the viscous sublayer is neglected as well as the layer situated over the zone for which the universal logarithmic law is usually used. It was also shown [1] that, by utilizing just two empiric constants, $n = 2/3$ and $k_n = 0.55$ for example, the new variant of the phenomenologic theory of the planar turbulent boundary layer permitted to recalculate and to reconfirm all 33 turbulent boundary layers, which were chosen as the reference at the Stanford Conference [2].

It is also to be noted that we have recently extended ([5],[7]) the phenomenologic theory by Novozilov to the case of axisymmetrical turbulent boundary layer.

2 Planar turbulent boundary layer

It is practically impossible to obtain equations of the turbulent boundary layer in a strict way, starting with the general Reynolds' equations. Therefore, we make use of an intuitive analogy with the laminar boundary layer by considering lower longitudinal derivatives with respect to those that are transversal and by replacing the second equation by a condition for the smallness of the normal gradient of the pressure relative to the longitudinal one. That is why the equations of the planar turbulent boundary layer are in the following form:

$$\bar{u}\frac{\partial \bar{u}}{\partial x} + \bar{v}\frac{\partial \bar{u}}{\partial y} = u_e u_e' + \frac{1}{\rho}\frac{\partial \tau t}{\partial y}, \qquad \frac{\partial \bar{u}}{\partial x} + \frac{\partial \bar{v}}{\partial y} = 0, \tag{1}$$

where:

(x, y) - usual orthogonal curvilinear coordinates,

$(\bar{u}, \bar{v})$ - velocity components at (x, y) in the boundary layer,

$u_o(x)$ - free-stream velocity,

$\tau_t = \mu\dfrac{\partial\bar{u}}{\partial y} - \rho\overline{u'v'} = \mu\dfrac{\partial\bar{u}}{\partial y} + \tau$ - global turbulent stress containing in principle a viscous part as well as turbulent one.

If the viscous part of the global stress is neglected then the system of equations (1) reduces to:

$$\frac{1}{\rho}\frac{\partial\tau}{\partial y} = -u_e u_e' + \bar{u}\frac{\partial\bar{u}}{\partial x} + \bar{v}\frac{\partial\bar{u}}{\partial y}, \qquad \frac{\partial\bar{u}}{\partial x} + \frac{\partial\bar{v}}{\partial y} = 0. \tag{2}$$

Or, due to the rheological power law and the Prandtl turbulence model chosen herein, it results that:

$$\frac{1}{\rho}\tau = \nu k_n T^n \frac{\partial\bar{u}}{\partial y}, \tag{3}$$

$$T = \frac{y^2}{\nu}\left|\frac{\partial\bar{u}}{\partial y}\right|. \tag{4}$$

The system of equations (2) must be resolved for the following boundary conditions:

$$\begin{aligned} \bar{u} &= \bar{v} = 0, \qquad \frac{\partial\bar{u}}{\partial y} \to \infty \qquad \text{for} \qquad y = 0, \\ \bar{u} &= u_e(x), \qquad \tau = 0 \qquad \text{for} \qquad y = \delta(x), \end{aligned} \tag{5}$$

as well as for the next initial condition:

$$\bar{u} = u_o(y) \qquad \text{for} \qquad x = x_o, \tag{6}$$

where $\delta(x)$ is the thickness of the boundary layer.

In order to calculate the turbulent boundary layer, we use in practice most often an integral relation obtained from the system of equations (2), called the momentum equation, in the following form:

$$\frac{d\delta_2}{dx} + \frac{u_e'\delta_2}{u_e}(2 + H) = \frac{1}{2}c_f, \tag{7}$$

where:

$$\delta_1(x) = \int_0^{\delta} \left(1 - \frac{\bar{u}}{u_e}\right) dy, \qquad \delta_2(x) = \int_0^{\delta} \frac{\bar{u}}{u_e}\left(1 - \frac{\bar{u}}{u_e}\right) dy,$$
$$c_f = \frac{2\tau_o}{\rho \cdot u_e^2}, \qquad H = \frac{\delta_1}{\delta_2}. \tag{8}$$

Finally, if the unknown variable $\bar{v}$ is eliminated from the system of equations (2) by using:

$$\bar{v} = -\int_0^y \frac{\partial \bar{u}}{\partial x} dy, \tag{9}$$

then it results:

$$\frac{1}{\rho}\frac{\partial \tau}{\partial y} = -u_e u_e' + \bar{u}\frac{\partial \bar{u}}{\partial x} - \frac{\partial \bar{u}}{\partial y}\int_0^y \frac{\partial \bar{u}}{\partial x} dy. \tag{10}$$

2.1 Generalization of the Falkner-Skan equation

Let the velocity $u_e(x)$ at the external frontier of the boundary layer be given by:

$$u_e(x) = C(x - x_o)^m, \tag{11}$$

where C, x_o and m are constants. If nondimensional coordinates are introduced as:

$$\bar{x} = \frac{U_o \cdot x}{\nu}, \qquad \bar{y} = \frac{U_o \cdot y}{\nu}, \tag{12}$$

then the constant U_o (having the dimension of the velocity) can be determined by the relationship:

$$u_e(x) = C(x - x_o)^m = U_o(\bar{x} - \bar{x}_o)^m \tag{13}$$

where:

$$\bar{x} = \frac{U_o \cdot x_o}{\nu}. \tag{14}$$

Besides, (12) and (13) yield:

$$U_o = \nu \frac{m}{1+m} C^{\frac{1}{1+m}}. \tag{15}$$

If a solution of the equation (10) is assumed in the form:

$$\bar{u} = U_o \left(\bar{x} - \bar{x}_o\right)^{\alpha-\beta} F'(\eta) \tag{16}$$

where:

$$\eta = \frac{\bar{y}}{\left(\bar{x} - \bar{x}_o\right)^{\beta}}, \tag{17}$$

with α and β being constants with numerical values to be determined in the sequel, then by replacing τ, T, u_e and $\bar{u}$ from (3), (4), (13) and (16), respectively, into the equation (10), and after carrying out several transformations, follows (18),

$$k_n \left(\bar{x} - \bar{x}_o\right)^{\alpha(1+n)-3\beta} \cdot \left(t^n F''\right)' =$$

$$= \left(\bar{x} - \bar{x}_o\right)^{2(\alpha-\beta)-1} (\alpha - \beta) F'^2 - \alpha F F'' - m \left(\bar{x} - \bar{x}_o\right)^{2m-1}. \tag{18}$$

It is evident that the conditions for the separation of the variables $\bar{x}$and η in the equation (18) are given by (19),

$$\alpha - \beta = m, \qquad \alpha(1+n) - 3\beta = 2m - 1, \tag{19}$$

hence α and β are determined in terms of parameters n and m,

$$\alpha = \frac{1+m}{2-n}, \qquad \beta = \frac{1+m}{2-n} - m. \tag{20}$$

For such values of α and β, the equation (18) reduces to an ordinary differential equation,

$$k_n \left(t^n F''\right)' = -\frac{1+m}{2-n} F F'' - m\left(1 - F'^2\right), \tag{21}$$

where:

$$t = \eta^2 F'', \tag{22}$$

which should be solved for the following boundary conditions:

$$\begin{aligned} F &= F' = 0, \qquad F'' \to \infty \qquad \text{for} \qquad \eta = 0, \\ F' &= 1, \qquad t^n F'' = 0 \qquad \text{for} \qquad \eta = \eta_o = constant. \end{aligned} \tag{23}$$

These conditions are derived by replacing (3), (4) and (16) into (5).

It is to be noted that for $n = 0$ and $k_n = 1$, the equation (21) becomes the well known one by Falkner-Skan in the case of the laminar boundary layer. In other words, it is easy to verify that $n = 0$ and $k_n = 1$, the relationships (3) and (4) reduce to the newtonian laminar linear rheological law:

$$\frac{\tau}{\rho} = \nu \frac{\partial u}{\partial y}.$$

By integrating the equation (21) from $\eta = 0$ to $\eta = \eta_o$ we obtain the next algebraic equation:

$$c = \left(\frac{1+m}{2-n} + m \right) \overset{**}{\eta} + m \overset{**}{\eta}, \tag{24}$$

where $c, \overset{*}{\eta}$ and $\overset{**}{\eta}$ are coefficients dependent on m and n:

$$\begin{cases} \overset{*}{R} = \dfrac{u_e \delta_1}{\nu} = \overset{*}{\eta} (\bar{x} - \bar{x}_o)^{\frac{1+m}{2-n}}, \\ \overset{**}{R} = \dfrac{u_e \delta_1}{\nu} = \overset{**}{\eta} (\bar{x} - \bar{x}_o)^{\frac{1+m}{2-n}}, \\ c_f = 2c (\bar{x} - \bar{x}_o)^{-\frac{1-n}{2-n}(1+m)}. \end{cases} \tag{25}$$

These expressions should be completed with the relationship (26),

$$R_\delta = \frac{u_e \delta}{\nu} = \eta_o (\bar{x} - \bar{x}_o)^{\frac{1+m}{2-n}}, \tag{26}$$

which determines the thickness of the boundary layer.

The generalized Falkner-Skan's differential equation (21) was recently resolved [7] numerically for various pairs of values of n and k_n.

The following values are of the greatest significance for calculation of the turbulent boundary layers with pressure gradients:

$$n = 2/3, \qquad k_n = 0.55,$$

$$n = 3/4, \qquad k_n = 0.53.$$

It is to be noted finally that there exist also [7] tables of numerical values of coefficients appearing in the formulas (25) and (26): $c, \eta_o, \overset{*}{\eta}, \overset{**}{\eta}$ that correspond to various pairs of values n and k_n, and to various values of m.

Figure 1 determines the coefficient c used in the formula of the parietal stress (25), as a function of m and for various values of n.

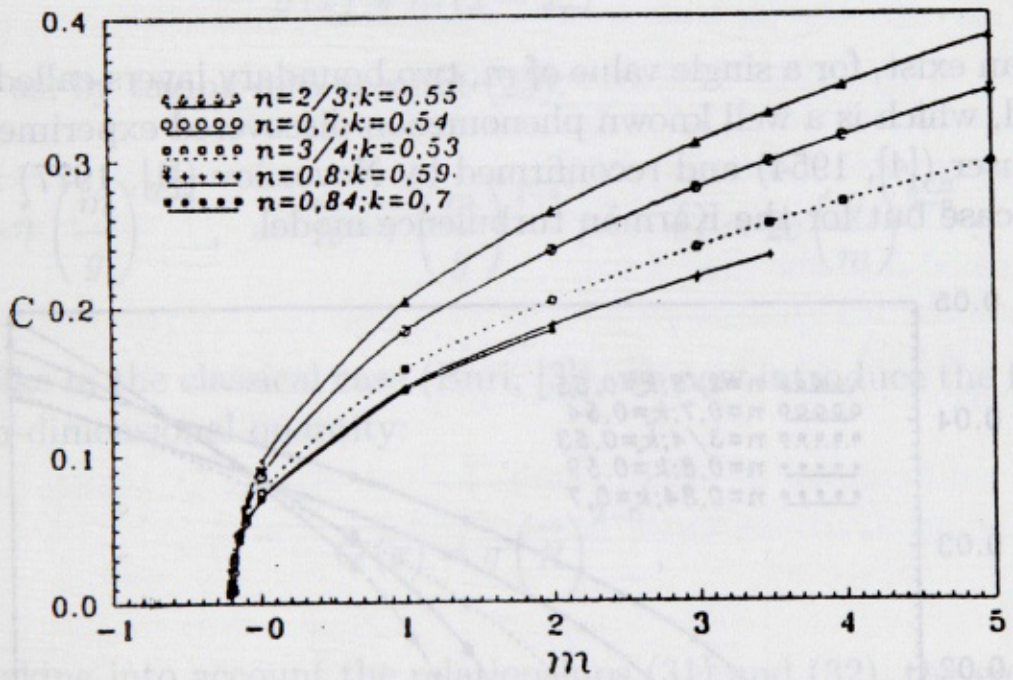

Fig. 1. Variation of shearing stress factor.

Evidently, for every pair of values of n and k_n, there exists a value $m = m_{\min}$ delimiting the existence domain of the solution of the considered case (called often the equilibrated boundary layer). Values of $m_{\min}$ depend a little of n and vary over the interval:

$$-0.2235 \leq m_{\min} \leq -0.1905. \tag{27}$$

The intersection points of the curves $c = f(m)$ and the axis m yield critical values of

$$m = m_{cr} < 0,$$

for which the parietal stress vanish, which announces the separation of the boundary layer.

Figure 2 shows that m_{cr} varies over the interval:

$$-0.2220 \leq m_{cr} \leq -0.1885. \tag{28}$$

A detailed analysis of the zone of negative values of m (Fig. 2) demonstrates that, over interval:

$$m_{\min} \leq m \leq m_{cr}, \tag{29}$$

there can exist, for a single value of m, two boundary layers called equilibrated, which is a well known phenomenon discovered experimentally by Clauser ([4], 1954) and reconfirmed by Novozilov ([1], 1977) in the analog case but for the Kàrmàn turbulence model.

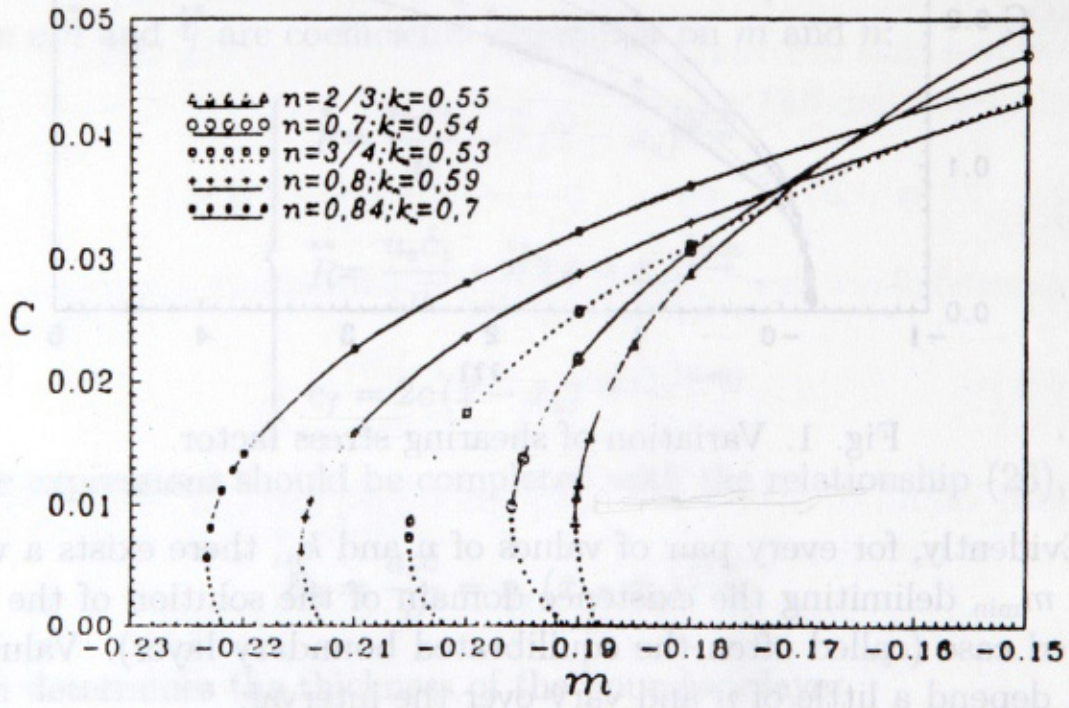

Fig. 2. Variation of shearing stress factor.

2.2 Practical approximate computing method of the turbulent boundary layer for arbitrary external velocity $u_e(x)$

An additional parameter is to be introduced at first,

$$g(x) = \frac{\nu}{u_e^2} u_e'. \tag{30}$$

After that, if we reconsider the case of the boundary layer called equilibrated, which was studied above in 2.1. and characterized by (11) and (14), then it is easy, by applying (30), to find out that

$$g(x) = m(\bar{x} - \bar{x}_o)^{-(1+m)}, \tag{31}$$

as well as, by taking into account (25):

$$\overset{*}{R} = \overset{*}{\eta} \left(\frac{m}{g}\right)^{\frac{1}{2-n}}, \qquad \overset{**}{R} = \overset{**}{\eta} \left(\frac{m}{g}\right)^{\frac{1}{2-n}}, \qquad c_f = 2c \left(\frac{g}{m}\right)^{\frac{1-n}{2-n}}. \tag{32}$$

If, like in the classical case (Buri, [3]), we now introduce the following non-dimensional quantity:

$$Q(x) = g \left(\overset{**}{R}\right)^{2-n}, \tag{33}$$

then, taking into account the relationships (31) and (32), the equation (33) reduces to (34),

$$Q(x) = g \left(\overset{**}{R}\right)^{2-n} = g \left[\overset{**}{\eta} \left(\frac{m}{g}\right)^{\frac{1}{2-n}}\right]^{2-n} = m \left(\overset{**}{\eta}\right)^{2-n}, \tag{34}$$

hence: $\overset{**}{\eta} = (Q/m)^{\frac{1}{2-n}}$, that is that $\overset{**}{\eta}$ is function just of Q.

It is now suitable to note that the following two quantities are also

functions only of Q:

$$\begin{cases} c_f (R)^{1-n} = 2c \left(\frac{g}{m}\right)^{\frac{1-n}{2-n}} \left[\left(\overset{**}{\eta}\right)^{1-n} \left(\frac{m}{g}\right)^{\frac{1-n}{2-n}}\right] = 2c \left(\overset{**}{\eta}\right)^{1-n} = G(Q), \\ H = \frac{\delta_1}{\delta_2} = \frac{\overset{*}{\eta}}{\overset{**}{\eta}} = H(Q). \end{cases} \tag{35}$$

Both equations (35) are exactly valid only for the equilibrated boundary layers considered in 2.1, but they may be accepted as approximately valid for a more general case for which $u_e(x)$ is arbitrary function. It is to be noted that in the case of the local Reynolds number of the Kàrmàn form, the same hypothesis is very well justified [1].

In this case, the parameters δ_2, c_f and H will be therefore expressed in terms of two quantities: a parameter g given by (30) and another unknown parameter Q. Or, a differential equation for the determination of the parameter Q can be obtained by replacing the expressions (35) in the integral equation of the momentum quantity (7), which is at first transformed into the next form:

$$\frac{1}{2-n}\frac{d}{dx}\left(\overset{**}{R}\right)^{2-n} + (1+H)\frac{u_e \cdot g}{\nu}\left(\overset{**}{R}\right)^{2-n} = \frac{1}{2}\frac{u_e \cdot c_f}{\nu}\left(\overset{**}{R}\right)^{1-n}. \tag{36}$$

Hence, a differential equation results for calculating Q, taking into account the arbitrariness of the form of the function $u_e(x)$:

$$\frac{dQ}{dx} + E(Q)\frac{u_e'}{u_e}Q = \frac{u_e''}{u_e'}Q, \tag{37}$$

where:

$$E(Q) = (2-n)\left\{[1+H(Q)]\,Q - \frac{1}{2}G(Q)\right\} + 2Q. \tag{38}$$

It is to be noticed that the function $E(Q)$ depends on n, not only explicitly, but also through functions $G(Q)$and $H(Q)$, the forms of which depend on n and can be determined with help of numerical tables

of equilibrated boundary layers. In this sense, it is possible to ascertain that for every particular value of n, there is "its proper equation" (37) and "its proper formula" (38).

As numerous calculations of plane turbulent boundary layers, which are verified experimentally, demonstrated lately [1] in the case of the Kàrmàn turbulence model, the best agreement was obtained with the experimental results in the case in which $n = 2/3$ and $k_n = 0.55$ are taken to determine $E(Q)$. That is why, just to be able to compare our results, we are going to consider, in the sequel, the same case. In this particular case ($n = 2/3, k_n = 0.55$) and for the Prandtl turbulence model (4), we carried out detailed computations of the function $E(Q), G(Q)$ and $H(Q)$ with approximate analytical expressions of the next forms:

$$\begin{cases} E(Q) = -0.063 + 4.097Q - 23.163Q^2, \\ G(Q) = 0.0938 + 2.1143Q + 36.1035Q^2 + 984.7348Q^3, \\ H(Q) = 1.6529 - 2.17Q. \end{cases} \tag{39}$$

So, by inserting (39) into (37), or an approximate calculation of the turbulent boundary layer, in the case of $n = 2/3$, we obtain a Riccati like differential equation:

$$\frac{dQ}{dx} + \left(-0.063 + 4.097Q - 23.163Q^2\right)\frac{u'_e}{u_e} = \frac{u''_e}{u'_e}Q. \tag{40}$$

Nonetheless, this equation is not always very convenient for the calculation because of possible singularity due to the function u'_e through zero. Moreover, in the equation (40) there is also u''_e, the determination of which demands a double differentiation of the experimental curve $u_e(x)$, which causes very often significant errors. In order to avoid it, the unknown function in the equation (40) should be changed in the following way:

$$z = \frac{Q}{g}, \tag{41}$$

where:

$$z(x) = \left(\frac{**}{R}\right)^{4/3} = \left(\frac{u_e \delta_2}{\nu}\right)^{4/3}. \tag{42}$$

With the new unknown function $z(x)$ the equation (40) reduces to another Riccati like equation:

$$\frac{dz}{dx} - 23.163 \frac{\nu}{u_e^3} (u_e')^2 z^2 + 2.097 \frac{u_e'}{u_e} z = 0.063 \frac{u_e}{\nu}, \tag{43}$$

but this one is deprived of the mentioned inconveniencies. That is why the equation (43) is much more convenient for integration and used in the practice than (40).

It is to be noted finally that this method can be easily extended also [5] to the case of axially symmetric turbulent boundary layer on a body revolution, with the analogous differential equation for the function $z(x)$ as follows:

$$\frac{dz}{dx} - 23.163 \frac{\nu}{u_e^3} (u_e')^2 z^2 + \left(2.097 \frac{u_e'}{u_e} + \frac{4}{3} \frac{r'}{r}\right) z = 0.063 \frac{u_e}{\nu}, \tag{44}$$

where $r(x)$ denotes the radius of the sections taken at right angles to the axis.

As a consequence, the practical approximate method of computing the turbulent boundary layer proposed herein consists of the following steps to be done:

- At first, for a given distribution of the external velocity $u_e(x)$, the differential equations (43) or (44) are to be integrated, with a prescribed initial condition δ_2 for $x = x_1$:

$$z = \left(\frac{u_e \delta_2}{\nu}\right)^{4/3} = z_1 \qquad \text{for} \qquad x = x_1. \tag{45}$$

- After finding $z(x)$, determine the momentum thickness by using (46),

$$\delta_2(x) = \frac{\nu}{u_e} z^{3/4}, \tag{46}$$

as well as the parameter $Q(x)$ given by (30) and (41), i.e.

$$Q(x) = g(x)\, z(x)\,. \tag{47}$$

- The next step is to determine the functions $G(Q)$ and $H(Q)$ by using the relationships (39).

- The formulas:

$$H(x) = H(Q)\,, \qquad c_f(x) = z^{-1/4} G(Q)\,, \tag{48}$$

offer two particularly important characteristics of the turbulent boundary layer.

- Finally, by using the well known simplest idea, it will be possible to calculate an improved approximation of the mean velocity in the turbulent boundary layer by (49),

$$\frac{\bar{u}}{u_e} = \left[\frac{y}{\delta_2}\frac{H-1}{H(H+1)}\right]^{\frac{1}{2}(H-1)}, \tag{49}$$

where the functions $\delta_2(x)$ and $H(x)$ were determined beforehand by the formulas (46) and (48).

3 Application of the method

The practical approximate method developed above has been recently directly applied ([6], [7]) to several particular cases of the turbulent boundary layer. In order to illustrate the method, we are choosing herein just two examples.

3.1 The id. 2500 by P. Bradshow, Variant B ($u_e' < 0$)

In the case of the id. 2500 by P. Bradshow, variant B, the external velocity can be presented [2] by:

$$u_e(x) = 159.3x^{-0.15} \qquad ft/s. \tag{50}$$

Taking into account (50), we obtain the general solution of the differential equation of the Riccati type (43) in the next form:

$$z(x) = \frac{10^4}{0.0051} \frac{1.17848 + 0.0705 C x^{0.394}}{2.53164 + C x^{0.394}} x^{0.85},$$

which, after determining the integration constant in accordance with the initial condition (45): $C = -84.37263$, reduces to:

$$z(x) = 10^6 \frac{5.948 x^{0.394} - 1.178}{43.03 x^{0.394} - 1.290} x^{0.85}. \tag{51}$$

With the function $z(x)$ found in this way, the other characteristics of the boundary layer should be now calculated such as:

- at first, the momentum thickness (46):

$$\delta_2(x) = \frac{x^{0.15}}{102.115} 10^{-4} z^{3/4} \qquad /ft/ : \tag{52}$$

- then, with regard to (30) and (47), the next two parameters:

$$g(x) = -\frac{0.0147}{x^{0.85}} 10^{-5}, \qquad Q(x) = -\frac{0.0147 z(x)}{x^{0.85}} 10^{-5};$$

- finally, the formulas (39) and (48) offer $c_f(x)$ and $H(x)$.

The three characteristics particularly important for the turbulent boundary layer, which are so obtained and compared with experimentally found values [2] in deviation percentage are given in the Table 1.

Table 1: Turbulent boundary layer characteristics and their comparison with experimental values.

x /ft/	$Q(x)$	$G(Q)$	$z(x)$	$\delta_2(x)$ /inches/	$\delta_{2\,\mathrm{exp}}$	%
2.0	-0.0177	0.0625	216445.48	0.131	0.131	0
4.0	-0.0183	0.0611	404618.32	0.232	0.223	4
5.5	-0.0185	0.0607	537385.80	0.301	0.288	5
7.0	-0.0187	0.0604	665416.02	0.367	0.353	4

Table 1: (Continuation)

$x\ /ft/$	$c_f(x)$	$c_{f\,\mathrm{exp}}$	%	$H(x)$	H_{exp}	%
2.0	0.0026	0.0022	18	1.691	1.43	18
4.0	0.0024	0.0021	14	1.693	1.39	21
5.5	0.0022	0.0020	10	1.693	1.39	21
7.0	0.0021	0.0019	11	1.694	1.40	20

We calculate also the profile of the mean velocity and the distribution of the turbulent stress in the boundary layer at the point $x = 7\ ft$, with the aid of the formulas (3), (4) and (16):

$$\tilde{u} = F'\left(2.005\frac{y}{\delta}\right), \tag{53}$$

$$\frac{\tau \cdot 10^3}{\rho \cdot u_e^2} = 28.86\left(\frac{y}{\delta}\right)^{4/3} F''\left(2.005\frac{y}{\delta}\right)\left[F''\left(2.005\frac{y}{\delta}\right)\right]^{2/3}, \tag{54}$$

hence the Table 2 and the corresponding figures 3 and 4.

Table 2: Mean velocity profile and turbulent stress distribution in the boundary layer.

y/δ	0.1	0.2	0.3	0.4	0.5
$\tilde{u}$	0.48	0.64	0.75	0.83	0.89
$\frac{\tau \cdot 10^3}{\rho \cdot u_e^2}$	1.437	1.625	1.589	1.402	1.121

Table 2: (Continuation)

y/δ	0.6	0.7	0.8	0.9	1.0
$\tilde{u}$	0.93	0.96	0.98	0.99	1.0
$\frac{\tau \cdot 10^3}{\rho \cdot u_e^2}$	0.807	0.509	0.261	0.089	0.01

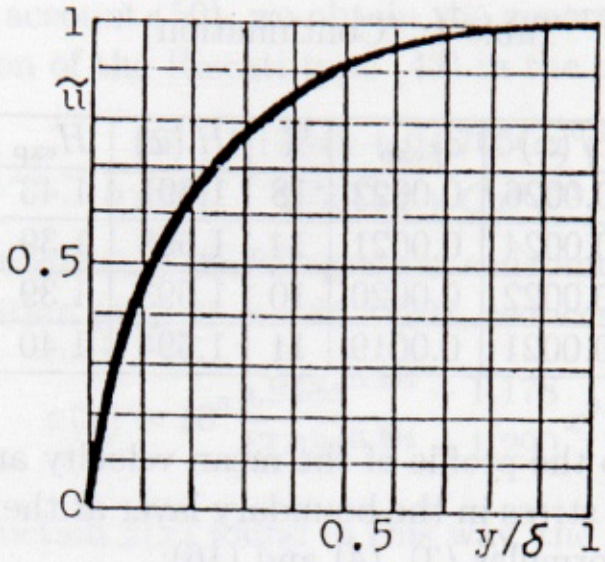

Fig. 3. Mean velocity profile.

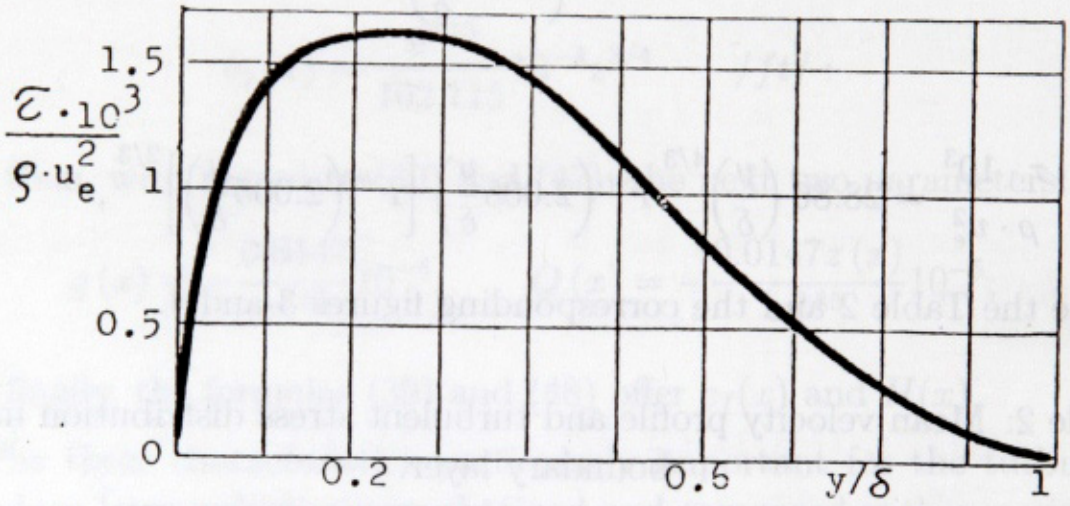

Fig. 4. Turbulent stress distribution.

3.2 Turbulent boundary layer on a sphere

In the case of a sphere of the radius R (Fig. 5), we have:

$$u_e(x) = \frac{3}{2} U_\infty \sin\frac{x}{R}, \qquad r(x) = R\sin\frac{x}{R}. \tag{55}$$

To integrate the differential equation (44), we should prescribe the initial condition (45). first of all, using the well known formula for

laminar momentum thickness:

$$\frac{u_e\delta_2^2}{\nu} = \frac{0.47}{r^2u_e^5}\int_0^x r^2u_e^5dx,$$

and taking account of (55), we calculate:

$$\left(\frac{\delta_2}{D}\right)^2 = \frac{0.235}{R_e}\left[\frac{32}{105}\frac{1}{\left(\sin\frac{x}{R}\right)^8} - \frac{48}{105}\frac{\cos\frac{x}{R}}{\left(\sin\frac{x}{R}\right)^8} + \frac{16}{105}\frac{\left(\cos\frac{x}{R}\right)^3}{\left(\sin\frac{x}{R}\right)^8}\right.$$

$$\left. - \frac{4}{35}\frac{\cos\frac{x}{R}}{\left(\sin\frac{x}{R}\right)^4} - \frac{2}{21}\frac{\cos\frac{x}{R}}{\left(\sin\frac{x}{R}\right)^2}\right]. \tag{56}$$

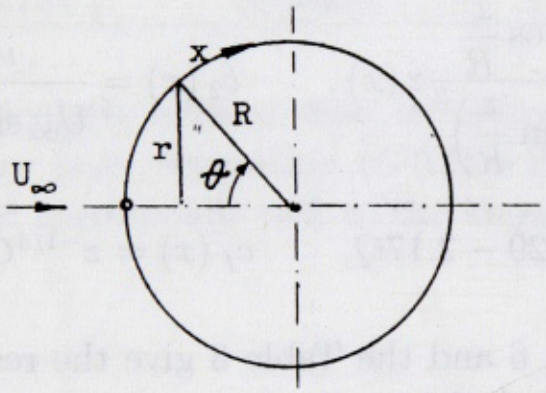

Fig. 5. Flow past a sphere.

If we suppose that the point of flow transition corresponds approximately to the point of pressure minimum: $x/R = \theta = 75^o$ experimentally ($\theta = 90^o$ theoretically) then from (45), taking account of (56), we obtain:

$$z = 0.206R_e^{2/3} \qquad \text{for} \qquad \theta = 75^o \tag{57}$$

In the particular case: $D = 2R = 0.5\ m, U_\infty = 5\ m/s, \nu = 1.52 \cdot 10^{-5}\ m^2/s$, the differential equation (44), presented in the form:

$$\frac{dz}{dx} - \frac{123.536}{R_e}\frac{\left(\cot\frac{x}{R}\right)^2}{\sin\frac{x}{R}}z^2 + 13.72\left(\cot\frac{x}{R}\right)z = 0.189R_e\sin\frac{x}{R}, \tag{58}$$

was integrated numerically, for the initial condition resulted from (57):

$$z = z_1 = 617.78 \qquad \text{for} \qquad \theta = 75^o,$$

with

$$R_e = \frac{U_\infty D}{\nu} = 1.6447 \cdot 10^5.$$

This numerical solution $z(x)$, together with the parameter $g(x)$ obtained from (30) in the following form:

$$g(x) = \frac{4}{3R_e}\left(\cos\frac{x}{R}\right)\left(\sin\frac{x}{R}\right)^{-2},$$

give then the parameter $Q(x)$ given by (47), as well as other turbulent boundary layer characteristics on a sphere according to (46) and (48):

$$\begin{cases} Q(x) = \dfrac{4}{3R_e}\dfrac{\cos\dfrac{x}{R}}{\left(\sin\dfrac{x}{R}\right)^2} z(x), \qquad \delta_2(x) = \dfrac{\nu}{U_\infty \sin\dfrac{x}{R}} z^{3/4}, \\ \\ H(x) = 1.6529 - 2.17Q, \qquad c_f(x) = z^{-1/4} G(Q). \end{cases} \tag{59}$$

The enclosed Fig. 6 and the Table 3 give the results of the corresponding numerical analysis.

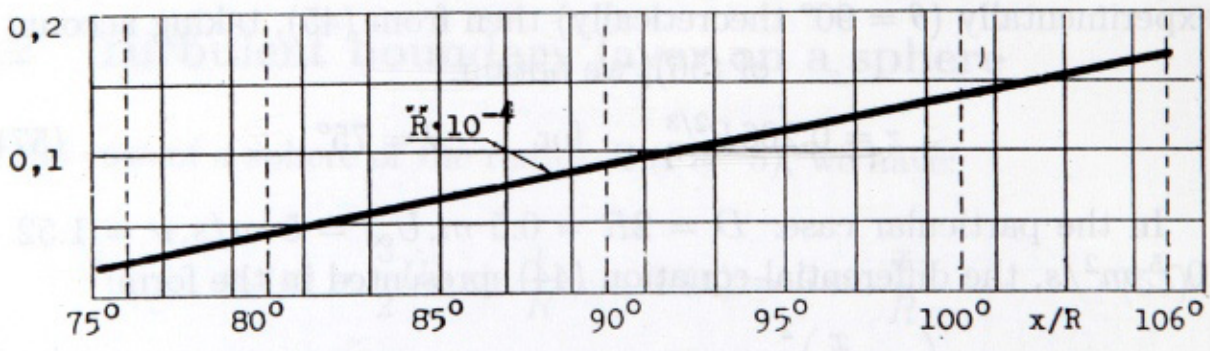

Fig. 6. Dimensionless momentum thickness on a sphere.

Table 3: Turbulent boundary layer characteristics on a sphere.

$x/R\,(^o)$	$z\,(x)$	$\left(\frac{u_e\delta_2}{\nu}\right) 10^{-4} = \overset{**}{R} \cdot 10^{-4}$	$H\,(x)$	$c_f\,(x)$
76	1129.726	0.01949	1.64779	0.01783
80	3148.645	0.04203	1.64298	0.01451
85	5674.332	0.06538	1.64413	0.01237
90	8299.815	0.08696	1.65290	0.01029
95	11146.680	0.10848	1.67012	0.00810
100	14395.666	0.13142	1.69824	0.00055
105	18366.398	0.15777	1.74253	0.00026
106	19294.721	0.16371	1.75415	-0.00186

It will be particularly noticed that, according to the Table 3, the turbulent boundary layer separation ($G\,(Q) = 0$) on a sphere occurs at $\theta = 106^o$, what corresponds well to the known experimental value ($\theta = 110^o$).

4 The evolution of the velocity profile in the neighborhood of the separation point

It is known that the situation is the following in the neighborhood of the separation point:

- upstream the separation point D, the mean velocity profile has the typical form of parietal flows (Fig. 3 or the curve 1 in the Fig. 7);

- downstream the separation point D, the velocity profile takes on rapidly the typical form of free flows (Fig. 7 - the curve 2),

- while the turbulent stress conserves practically the same pace, without undergoing great changes (Fig. 8 - full curve, analogously to the curve from Fig. 4) in the neighborhood of the separation point of

the boundary layer.

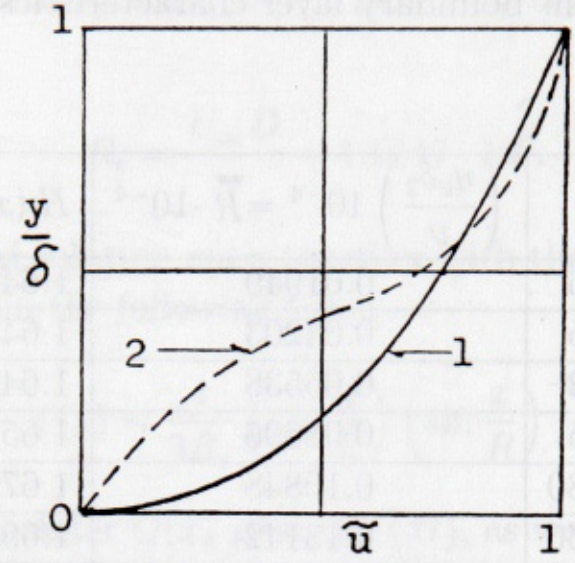

Fig. 7. Velocity profile evolution.

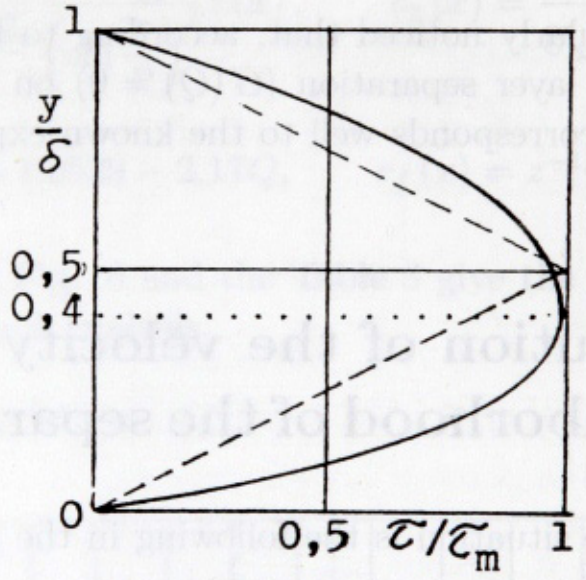

Fig. 8. Typical turbulent stress distribution.

We are going to study, and to compare with experimental results, the velocity profile at the boundary layer in two sections: Section I BEFORE D and Section II AFTER D - in two approximate variants: triangular (pointed segments in the Fig. 8) and parabolic variant (two parabolic segments in the Fig. 8).

4.1 Section I - UPSTREAM D

4.1.1 Triangular variant

If the maximum value of the Reynolds turbulent stress is designated by τ_m, then the equations of two pointed straight segments (Fig. 8) are:

$$\tau = 2\tau_m \frac{y}{\delta}, \qquad 0 \le y \le \delta/2, \tag{60}$$

$$\tau = 2\tau_m \left(1 - \frac{y}{\delta}\right), \qquad \delta/2 \le y \le \delta. \tag{61}$$

By combining the chosen power law (3), in the case of the Prandtl turbulent model (4) and for the next values of two constants: $n = 2/3$ and $k_n = 0.55$:

$$\tau = \rho k_n \nu^{1/3} y^{4/3} \left|\frac{d\bar{u}}{dy}\right|^{5/3},$$

with the expressions (60) and (61), it is found:

$$k_n \nu^{1/3} \left|\frac{d\bar{u}_1}{dy}\right|^{5/3} = 2\frac{\tau_m}{\rho}\frac{y}{\delta} y^{-4/3}, \qquad 0 \le y \le \delta/2, \tag{62}$$

$$k_n \nu^{1/3} \left|\frac{d\bar{u}_2}{dy}\right|^{5/3} = 2\frac{\tau_m}{\rho}\left(1 - \frac{y}{\delta}\right) y^{-4/3}, \qquad \delta/2 \le y \le \delta. \tag{63}$$

The boundary conditions for the differential equations (62) and (63), in the concerning domains, are the following:

$$\begin{cases} \bar{u}_1 = 0 & \text{for} \quad y = 0; \\ \bar{u}_1 = \bar{u}_2, \quad d\bar{u}_1/dy = d\bar{u}_2/dy & \text{for} \quad y = \delta/2; \\ \bar{u}_2 = u_e & \text{for} \quad y = \delta. \end{cases} \tag{64}$$

By introducing now dimensionless quantities:

$$\tilde{u} = \frac{\bar{u}}{u_e}, \qquad \tilde{\tau}_m = \frac{\tau_m}{\rho \cdot u_e^2}, \qquad \eta = \frac{y}{\delta}, \tag{65}$$

the equations (62) and (63) can be reduced to:

$$\frac{d\tilde{u}_1}{d\eta} = A^{3/5}\eta^{-1/5} \qquad 0 \le \eta \le 1/2, \tag{66}$$

$$\frac{d\tilde{u}_2}{d\eta} = A^{3/5}\,(1-\eta)^{3/5}\,\eta^{-4/5}, \qquad 1/2 \le \eta \le 1, \tag{67}$$

where:

$$A = \frac{2}{k_n}\tilde{\tau}_m R_\delta^{1/3} \qquad \text{and} \qquad R_\delta = \frac{u_e \cdot \delta}{\nu}. \tag{68}$$

The boundary layer conditions (64) become:

$$\begin{cases} \tilde{u}_1 = 0 & \text{for} \quad \eta = 0, \\ \tilde{u}_1 = \tilde{u}_2, \quad d\tilde{u}_1/d\eta = d\tilde{u}_2/d\eta & \text{for} \quad \eta = 1/2, \\ \tilde{u}_2 = 1 & \text{for} \quad \eta = 1. \end{cases} \tag{69}$$

At first, it is easy to conclude by comparing (66) and (67) that:

$$d\tilde{u}_1/d\eta = d\tilde{u}_2/d\eta \qquad \text{for} \qquad \eta = 1/2.$$

Afterwards, by integrating the differential equation (66):

$$\tilde{u}_1 = \frac{5}{4}A^{3/5}\eta^{4/5} + C_1,$$

with the integration constant, according to (69), equals zero: $C_1 = 0$, the solution is obtained as:

$$\tilde{u}_1 = \frac{5}{4}A^{3/5}\eta^{4/5}, \qquad 0 \le \eta \le 1/2. \tag{70}$$

At last, from (67) it results that:

$$\tilde{u}_2 = A^{3/5}\int (1-\eta)^{3/5}\,\eta^{-4/5}d\eta + C_2.$$

But, by the Tchebichef theorem, the last integral of the differential binomial cannot be expressed by elementary functions, and we are going to find it, for a moment, in an approximate form of a serial expansion:

$$\tilde{u}_2 = A^{3/5}\left(5\eta^{1/5} - \frac{1}{2}\eta^{6/5} - \frac{3}{55}\eta^{11/5} - \frac{7}{400}\eta^{16/5}\right) + C_2. \tag{71}$$

The integration constant will be calculated by using (69), that is that: $\tilde{u}_2 = 1$ for $\eta = 1$, in the form:

$$C_2 = 1 - \frac{19483}{4400}A^{3/5},$$

so that (71) reduces to:

$$\tilde{u}_2 = 1 - A^{3/5}\left(\frac{19483}{4400} + \frac{7}{400}\eta^{16/5} + \frac{3}{55}\eta^{11/5} + \frac{1}{2}\eta^{6/5} - 5\eta^{1/5}\right), \quad \frac{1}{2} \leq \eta \leq 1. \tag{72}$$

If the last condition (69) is utilized: $\tilde{u}_1 = \tilde{u}_2$ for $\eta = 1/2$, taking into account (70) and (72), then the value of the parameter A results:

$$A = 0.96038, \tag{73}$$

or, in view of the relationship (68):

$$\tilde{\tau}_m \cdot R_\delta^{1/3} = 0.264. \tag{74}$$

Hence, by combining (73), (70) and (72), the final formulas of the velocity profile will be obtained over the concerned domains:

$$\tilde{u}_1 = 1.22\eta^{4/5}, \qquad 0 \leq \eta \leq 1/2; \tag{75}$$

$$\tilde{u}_2 = 4.88\eta^{1/5} - 0.01708\eta^{16/5} - 0.05324\eta^{11/5} - 0.488\eta^{6/5} - 3.32168, \quad 1/2 \leq \eta \leq 1. \tag{76}$$

If it is chosen, in order to test the procedure, a typical case of the pre-separation of the boundary layer - the last section ($x = 4.926\ ft$) of the id. 3500 of B.G. Newman ([2], 1968), with $u'_e < 0$, then, as the Table 4 and Fig. 9 show, sufficiently satisfactory results are obtained since the deviation is not larger than about 17%.

Table 4: Velocity profile compared with the experiment.

	0.00	0.05	0.10	0.20	0.30	0.40
According to (70)	0.00	0.111	0.193	0.337	0.466	0.586
Newman's experiment	0.00	0.115	0.210	0.300	0.400	0.500
Deviation (%)	0	3.5	8	12	16	17

Table 4: (continuation)

	0.50	0.60	0.70	0.80	0.90	1.00
According to (71)	0.701	0.799	0.874	0.931	0.972	1.00
Newman's experiment	0.610	0.710	0.810	0.900	0.960	1.00
Deviation (%)	15	12	8	3	1	0

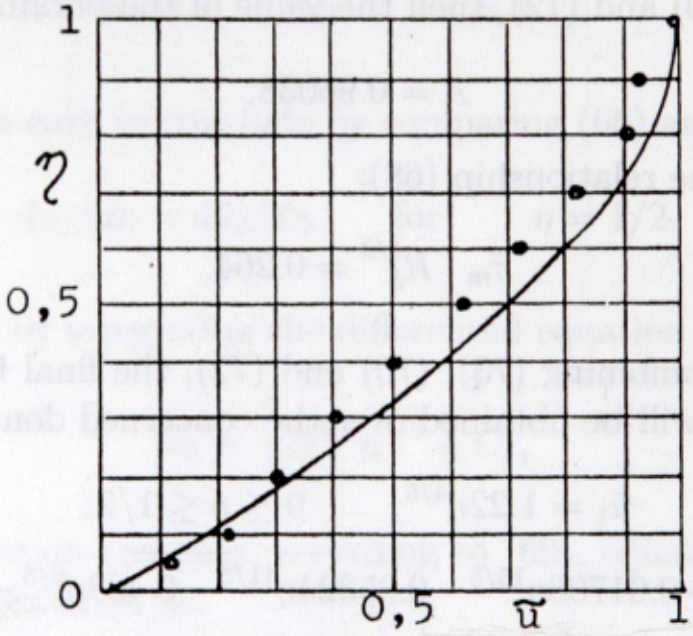

Fig. 9. Velocity profile upstream D.

An experimental verification of the formula:

$$\tilde{\tau}_m \cdot R_\delta^{1/3} = const. = \frac{1}{2} k_n A = 0.275A \qquad (77)$$

is highly difficult in the case of the boundary layers with separation, so that almost nobody measured the turbulent stress in the section. The unique exception presents the id. 2100 by Schubauer and Klebanoff ([2], 1968), where the separation point appears at:

$$x = 25.77\ ft,$$

with the next parameter values which are necessary to calculate the left-hand side of the relationship (77):

$$u_e = 112\ ft/s, \qquad \delta = 8.1\ inch,$$

$$\tilde{\tau}_m = 0.005, \qquad \nu = 1.6 \cdot 10^{-4}\ ft^2/s.$$

As a consequence, it is obtained that:

$$\tilde{\tau}_m \cdot R_\delta^{1/3} = \tilde{\tau}_m \left(\frac{u_e \cdot \delta}{\nu} \right)^{1/3} = 0.005 \left(\frac{112 \cdot 8.1 \cdot 0.0833}{1.6 \cdot 10^{-4}} \right)^{1/3} = 0.389,$$

Then from (77) results that:

$$A = 1.41454, \tag{78}$$

which makes a difference of 33% with respect to the theoretical solution (73), found above. It is possible to say that such an agreement is even acceptable in spite of the deficiency of the experimental results to enable general conclusions.

4.1.2 Parabolic variant

The results obtained above by using a triangular approximate schematization of the Reynolds stress being satisfactory, should be nevertheless improved by using the shapes closer to experimental ones, which are the following (Fig. 8):

$$\frac{\tau}{\tau_m} = \begin{cases} f_1(\eta) = 5\eta\,(1 - 1.25\eta), & 0 \le \eta \le 0.4, \\ f_2(\eta) = \dfrac{10}{3}\,(1-\eta)\left[1 - \dfrac{5}{6}\,(1-\eta)\right], & 0.4 \le \eta \le 1. \end{cases} \tag{79}$$

Repeating the same type of the reasoning as in 4.1.1., the problem, which we are studying - reduces to the next differential equations:

$$\frac{d\tilde{u}_1}{d\eta} = 0.65975 A^{3/5} \eta^{-4/5} \left[f_1(\eta)\right]^{3/5}, \quad 0 \leq \eta \leq 0.4; \tag{80}$$

$$\frac{d\tilde{u}_2}{d\eta} = 0.65975 A^{3/5} \eta^{-4/5} \left[f_2(\eta)\right]^{3/5}, \quad 0.4 \leq \eta \leq 1, \tag{81}$$

with the boundary conditions, respectively:

$$\begin{cases} \tilde{u}_1 = 0 \quad \text{for} \quad \eta = 0; \\ \tilde{u}_1 = \tilde{u}_2, \quad d\tilde{u}_1/d\eta = d\tilde{u}_2/d\eta \quad \text{for} \quad \eta = 0,4; \\ \tilde{u}_2 = 1 \quad \text{for} \quad \eta = 1. \end{cases} \tag{82}$$

4.2 Section II - DOWNSTREAM D

The evolution of the velocity profile around the separation point of the boundary layer with respect to the Figure 7: the curve 1 - before D, and the curve 2 - after D, the turbulent stress conserving practically the same shape, in fact, is such an evolution of the velocity profile that leads to an idea that the boundary layer equations admit two solutions in the neighborhood of the separation point: one before and another after the point.

According to the relationships (66) and (67) (based evidently on a triangular approximate schematization), the expressions characterizing the curvature of the velocity profile in the concerned domains are the following:

$$\frac{d^2\tilde{u}_1}{d\eta^2} = -\frac{1}{5} A^{3/5} \eta^{-6/5}, \quad 0 \leq \eta \leq \frac{1}{2}$$

$$\frac{d^2\tilde{u}_2}{d\eta^2} = -\frac{1}{5} A^{3/5} \left[3(1-\eta)^{-2/5} \eta^{-4/5} + 4(1-\eta)^{3/5} \eta^{-9/5}\right], \quad \frac{1}{2} \leq \eta \leq 1.$$

Now, taking into account that, in the Section I - BEFORE D, $d^2\tilde{u}_2/d\eta^2$ preserves practically its sign in the whole interval $0 \leq \eta \leq 1$, while

in the Section II - AFTER D, $d^2\tilde{u}_2/d\eta^2$ changes its sign into $\eta = 1/2$, so that the above equations should be readapted for every of the two sections in the following way:

$$\frac{d^2\tilde{u}_1}{d\eta^2} = \mp\frac{1}{5}A^{3/5}\eta^{-6/5}, \quad 0 \leq \eta \leq \frac{1}{2}, \tag{83}$$

$$\frac{d^2\tilde{u}_2}{d\eta^2} = -\frac{1}{5}A^{3/5}\left[3\,(1-\eta)^{-2/5}\,\eta^{-4/5} + 4\,(1-\eta)^{3/5}\,\eta^{-9/5}\right], \quad \frac{1}{2} \leq \eta \leq 1. \tag{84}$$

The upper signs of the second terms correspond to Section I - BEFORE D, which has been already treated in the 4.1; the lower signs are attributed to the Section II - AFTER D.

As a consequence, it still remains to explore solutions of the equations (83) and (84) concerning the lower signs, namely:

$$\frac{d^2\tilde{u}_1}{d\eta^2} = \frac{1}{5}A^{3/5}\eta^{-6/5}, \quad 0 \leq \eta \leq \frac{1}{2}, \tag{85}$$

$$\frac{d^2\tilde{u}_2}{d\eta^2} = -\frac{1}{5}A^{3/5}\left[3\,(1-\eta)^{-2/5}\,\eta^{-4/5} + 4\,(1-\eta)^{3/5}\,\eta^{-9/5}\right], \quad \frac{1}{2} \leq \eta \leq 1. \tag{86}$$

with the following boundary conditions:

$$\begin{cases} \tilde{u}_1 = 0 \quad \text{for} \quad \eta = 0, \\ \tilde{u}_1 = \tilde{u}_2, \quad d\tilde{u}_1/d\eta = d\tilde{u}_2/d\eta \quad \text{for} \quad \eta = \dfrac{1}{2}, \\ \tilde{u}_2 \quad \text{for} \quad \eta = 1. \end{cases} \tag{87}$$

After the first integration of the equations (85) and (86), it is obtained:

$$\frac{d\tilde{u}_1}{d\eta} = A^{3/5}\left(C_1 - \eta^{-1/5}\right), \tag{88}$$

$$\frac{d\tilde{u}_2}{d\eta} = A^{3/5}\left[C_2 + (1-\eta)^{3/5}\,\eta^{-4/5}\right], \tag{89}$$

from which by using the corresponding condition (87), namely:

$$d\tilde{u}_1/d\eta = d\tilde{u}_2/d\eta \quad \text{for} \quad \eta = 1/2,$$

follows the relationship between the integration constants:

$$C_1 = C_2 + 2^{6/5}. \tag{90}$$

The fact that the turbulent stress preserves practically the same shape before and after the separation point D has a consequence that the parameter A is conserving effectively after D the same value as before it, that is the value already found (73): $A = 0.96038$. By placing this value of A, as well as (90), in (88) and (89), it results that:

$$\frac{d\tilde{u}_1}{d\eta} = 0.97604\left[\left(C_2 + 2^{6/5}\right) - \eta^{-1/5}\right]; \tag{91}$$

$$\frac{d\tilde{u}_2}{d\eta} = 0.97604\left[C_2\,(1-\eta)^{3/5}\,\eta^{-4/5}\right]. \tag{92}$$

Carrying out, now, the second integration, at first of the differential equation (91):

$$\tilde{u}_1 = 0.97604\left[\left(C_2 + 2^{6/5}\right)\eta - \frac{5}{4}\eta^{4/5}\right] + C_{11}, \tag{93}$$

with $C_{11} = 0$ by taking into account that according to (87): $\tilde{u}_1 = 0$ for $\eta = 0$; then of the equation (92):

$$\tilde{u}_2 = 0.97604\left[(C_2\eta + J_2) + C_{22}\right], \tag{94}$$

where:

$$J_2(\eta) = \int (1-\eta)^{3/5}\,\eta^{-4/5}d\eta. \tag{95}$$

Calculating this integral once more in an approximate way, it is possible to deduce that:

$$J_2(1) = \frac{19483}{4400} \quad \text{and} \quad J_2\left(\frac{1}{2}\right) = 4.12134, \tag{96}$$

so that from the next condition: $\tilde{u}_2 = 1$ for $\eta = 1$, follows that:

$$C_{22} = -C_2 - J_2(1) + 1.02455 = -C_2 - 3.4034, \tag{97}$$

and (94) reduces to:

$$\tilde{u}_2 = 0.97604\left[C_2(1-\eta) + J_2(\eta) - 3.4034\right]. \tag{98}$$

Finally, the last of the conditions (87), that is: $\tilde{u}_1 = \tilde{u}_2$ for $\eta = 1/2$, taking into account the expressions (93) and (98), offers:

$$C_2 = J_2\left(\frac{1}{2}\right) - 3.83416 = 0.28718, \tag{99}$$

as well as, due to (97):

$$C_{22} = -3.69058. \tag{100}$$

As a consequence, by placing (99) and (100) into (93) and (98), the final solutions will be obtained in the domains concerned:

$$\tilde{u}_1 = 2.52265\eta - 1.22005\eta^{4/5}, \quad 0 \le \eta \le 1/2; \tag{101}$$

$$\begin{aligned}\tilde{u}_2 = {} & 0.2803\eta + 4.8802\eta^{1/5} - 0.48802\eta^{6/5} - 0.05324\eta^{11/5} - \\ & -0.01708\eta^{16/5} - 3.60215, \quad 1/2 \le \eta \le 1.\end{aligned} \tag{102}$$

The Figure 10 shows three profiles of the velocity in the boundary layer of the id. 3800 [2] of H.L. Moses (MIT Gas Turbine Laboratory, 1964; $u'_e < 0$) corresponding to points: $x_1 = 1.198\ ft$, $x_2 = 1.604\ ft$ and $x_3 = 2.083\ ft$.

It is evident that between the points x_1 and x_2 there is separation of the turbulent boundary layer, despite it is not mentioned in [6]. Hence, it is sure that point x_3 is in the separation zone. It is still to be noted that the probable shape of the velocity profile is sketched in Fig. 10 quite nearly to the wall at the points x_2 and x_3 where a revised flow exists ([1], [2]).

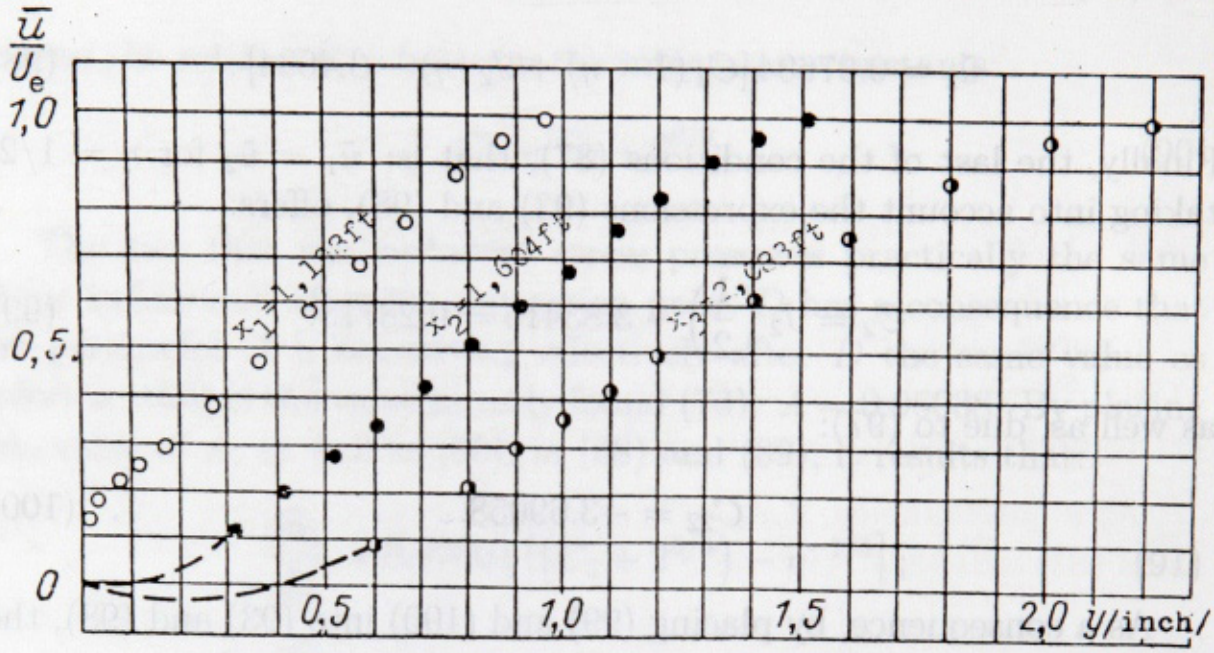

Fig. 10. Boundary layer velocity profiles, as measured by H. L. Moses.

The Table 5 and Fig. 11 present the results obtained by using the solutions (101) and (102) for one Section II - AFTER D, as well as the existing experimental results at the point x_3 of the id. 3800.

Table 5: Velocity profile compared with the experiment.

η	0	0.001	0.01	0.025	0.0375
According to (101)	0	-0.0023	-0.0054	-0.007	-0.0064
Experience by Moses	No experim. results				
Deviation (%)					

Table 5: (continuation)

η	0.10	0.20	0.30	0.40
According to (101)	0.0589	0.1679	0.291	0.422
Experience by Moses	0.075	0.180	0.280	0.420
Deviation (%)	20	7	4	1

Table 5: (continuation)

η	0.50	0.60	0.70	0.80	0.90	1.0
According to (102)	0.5606	0.6873	0.7904	0.8750	0.9441	1.0
Experience by Moses	0.520	0.650	0.770	0.850	0.930	1.0
Deviation (%)	8	6	3	3	1.5	0

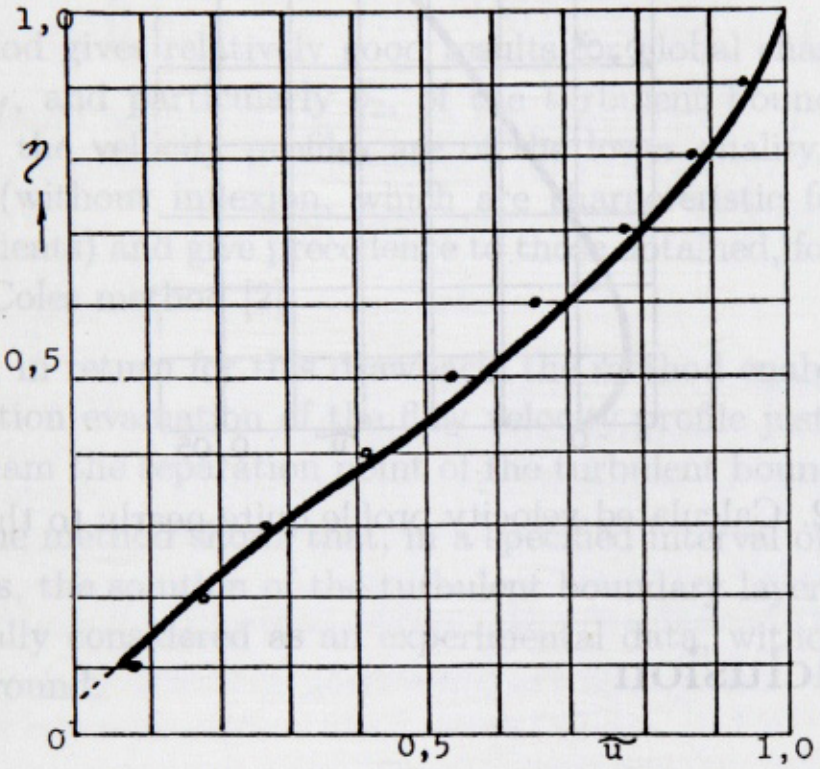

Fig. 11. Calculated velocity profile compared to the experimental results.

The Fig. 12 lays stress, in particular, on the numerical results of the Table 5 in the zone quite nearly to the wall. From there the minimum negative velocity quotient $\tilde{u} = \bar{u}/u_e$ is about the order of -0.005. Since for the id. 3800: $u_e = 40\ ft/s$ at the point $x_3 = 2.083\ ft$, the negative return velocities in the separation zone are therefore lower than $0.005 \cdot 40 = 0.2\ ft/s$, which is compatible with indication of the Fig. 10.

It is to be remarked, finally, that it is possible to envisage, of course, an improved solution, called a parabolic variant, by the analogy with

4.1.2, what we intend to do in the future.

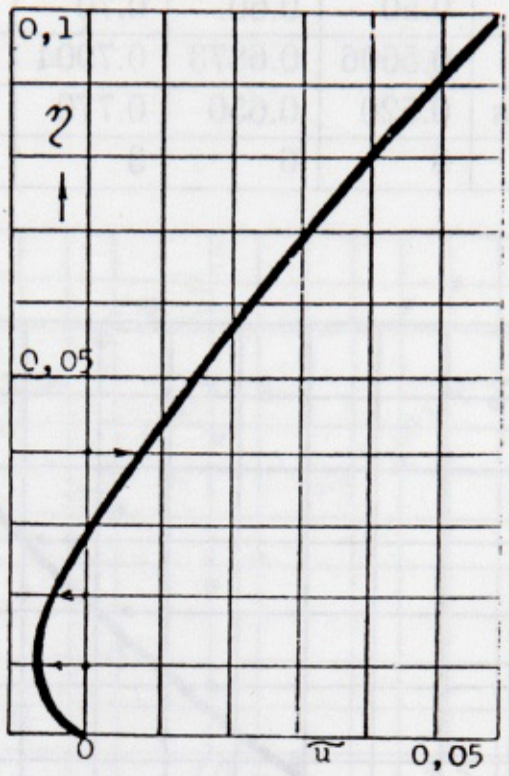

Fig. 12. Calculated velocity profile quite nearly to the wall.

5 Conclusion

As it is well known, the principle of the integral methods of the boundary layer computation, starting with the first such a method by Kàrmàn-Polhausen, is contained in an idea that it is not necessary to know the behavior of the velocity profile in details in order to get satisfactory practical results such as: the distribution of the displacement thickness δ_1, of the momentum thickness δ_2 ($H = \delta_1/\delta_2$) or of the wall friction coefficient c_f.

Just those quantities are interrelated in the Von Kàrmàn equation, which expresses the global force and momentum balance. Thus, in order to arrive to a relatively simple computation method, it is reasonable to begin not with the equation of the local momentum that describes the velocity change $\bar{u}$ itself, but with its integral form. In return, we must be satisfied with a certain approximation degree.

The same appears in this paper, by beginning with the integral equation of the momentum and with the analogy with the rheological power law, which is effectively used to study flows of non-newtonian liquids with nonlinear viscosities, a simple "one layer" practical method is obtained for an approximate computation of the turbulent boundary layer in the case of the Prandtl model of turbulence, where for the process ending it is necessary to know only two empirical constants (for example, $n = 2/3$ and $k_n = 0.55$).

The method gives relatively good results for global characteristics δ_2, H and c_f, and particularly δ_2, of the turbulent boundary layer. As expected, the velocity profiles are of the lower quality, relatively schematized (without inflexion, which are characteristic for positive pressure gradients) and give precedence to those obtained, for example, by the D.E. Coles method [2].

Although, in return for this drawback, the method enables a satisfactory evolution evaluation of the flow velocity profile just upstream and downstream the separation point of the turbulent boundary layer.

Finally, the method shows that, in a specified interval of the exponent m values, the solution of the turbulent boundary layer is double, which is usually considered as an experimental data, without a theoretical background.

References

[1] Novozilov V.V., Plane turbulent boundary layer theory of an incompressible flow, (monography in Russian), Edition "Sudostroenie", Leningrad, 1977.

[2] Proceedings - Computation of turbulent boundary layers - AFOSR-IFP, Stanford Conference, 1968.

[3] Buri A., Eine Berechnungsgrundlage für die turbulente Grenzschicht bei beschleunigter und verzögerter Strömung, Diss., Zürich, 1931.

[4] Clauser F.H., Turbulent boundary layers in adverse pressure gradients, J. Aero. Sci., Vol. 21 (1954), 91-108.

[5] Askovic R., Sur une methode approchee de traiter la couche limite turbulente a symetrie de revolution, Communication presentee au 10eme Congres Francais de Mecanique, Paris (1991), T. 2p. 305.

[6] Askovic R., Solution approchee de la couche limite turbulente dans un diffuseur plan, Teorijska i primenjena mehanika, 20, Beograd (1994), 1-16.

[7] Askovic R., Contribution a l'etude de la couche limite turbulente, Rapport No 94/A/01 du Laboratoire de Mecanique des fluides de l' Universite de Valenciennes, juin 1994.

R. Ašković
Laboratoire de Mécanique des fluides
Université de Valenciennes
France

O transformaciji profila brzine u okolini tačke odvajanja turbulentnog graničnog sloja

U radu se, najpre, razvija jedna približna metoda za proračun ravanskog turbulentnog graničnog sloja, u smislu poznate fenomenološke poluempirijske teorije turbulentnih strujanja, zasnovane na analogiji sa strujanjima nenjutnovskih fluida nelinearnih stepenih reoloških zakona viskoznosti. Metoda je, potom, uporedjena sa poznatim i eksperimentalno proverenim rešenjem P. Bradshow-a (ident. 2500). Najzad, u radu se predlaže i jedan približan postupak za odredjivanje profila brzine u okolini tačke odvajanja turbulentnog graničnog sloja, u slučaju Prandtl-ovog modela turbulencije. Izvršeno je, takodje, poredjenje dobijenih rešenja sa postojećim eksperimentalnim rezultatima (H.L. Moses - ident. 3800), sa zadovoljavajućim slaganjem.